

# CARITAS UNIVERSITY AMORJI-NIKE, EMENE, ENUGU STATE Caritas Journal of Engineering Technology

**CJET, Volume 3, Issue 1 (2024)** 

Article History: Received: 10th April, 2024 Revised: 19th June, 2024 Accepted: 10th Jule, 2024

# Application of Optimized Photo-Fenton Process for The Degradation of Allura Red Dye in Process Textile Wastewater

Udemba, Chinenye Margaret<sup>1</sup> Ezeh, Ernest Mbamalu<sup>2\*</sup> Odinma, Stanley Chukwudindu<sup>3</sup>

<sup>1</sup>Department of Chemical Engineering, Caritas University Amorji Nike Enugu State, Nigeria

<sup>2</sup>Department of Chemical Engineering, Federal University Otuoke, Bayelsa State, Nigeria

<sup>3</sup>Department of Industrial Chemistry, Caritas University Amorji Nike Enugu State, Nigeria

\*Correspondence: <u>ezehem@fuotuoke.edu.ng</u> ORCID: <u>https://orcid.org/0000-0002-0164-9325</u>

# Abstract

This study, presents an optimized photo-Fenton process degradation of Allura red dye from textile process industrial wastewater, by the determination of optimal conditions for the photo-Fenton process to achieve maximum Allura red degradation. Water scarcity is a critical challenge and a cornerstone of sustainable progress. Meeting the growing demand for drinking water is essential for modern societal development. The photo-Fenton process is an effective method for the degradation of organic pollutants and dyes in wastewater. The effects of different parameters such as pH, concentration of hydrogen peroxide, concentration of iron (III) ions, and initial dye concentration on the degradation efficiency were investigated. A central composite design (CCD) was used to determine the optimal values of the parameters. The results showed that the maximum degradation of Allura red dye (96%) was achieved at pH 3.5, hydrogen peroxide concentration of 0.1 M, iron (III) ion concentration of 0.005 M, and initial dye concentration of 25 mg/. The mineralization of the dye was evaluated by measuring the total organic carbon (TOC) removal. The maximum TOC removal was found to be 76.2%. Therefore, the optimized photo-Fenton process was considered a promising method for the removal of Allura red dye from textile industry wastewater. The experimental model generated precise equations, providing valuable insights into the degradation process.

Keywords: Advanced oxidation process; Optimization; Photo-Fenton process; Degradation; Wastewater.

# 1.0 Introduction

The growing global concern for sustainable practices has fueled the development of alternative water reuse technologies, particularly in industry and agriculture [1]. Water quality is threatened by chemical pollutants like solvents, dyes, and heavy metals, leading to significant environmental and ecosystem concerns [2]. Water, essential for all living organisms, is vital in various aspects of life including drinking, household needs, recreation, and commerce. It is alarming that nearly 900 million people lack access to safe drinking water, resulting in approximately 1.5 million child deaths annually due to water-related diseases [3]. Water pollution is a major environmental problem caused by the release of industrial effluents into water bodies worldwide. Among the many pollutants that are discharged, synthetic dyes have gained significant attention due to their non-biodegradability and toxicity to living organisms.

Industrial textile dyeing and finishing processes are some of the major sources of water pollution globally. The discharge of untreated effluents from these processes into water bodies has adverse effects on aquatic life, the environment, and human health [4]. The textile industry is among the largest consumers of water, accounting for over 20% of global industrial water usage. It generates significant quantities of wastewater that contain high concentrations of organic compounds, salt, and heavy metals, including carcinogenic and toxic substances. Conventional physicochemical methods such as adsorption, membrane treatment, and coagulation-flocculation are frequently employed to treat textile wastewater. Nevertheless, these techniques are not effective in removing toxic organic compounds completely.

Alura red dye is a water-soluble anionic dye that is commonly used in the textile industry. It is synthetically prepared and belongs to the azo dye family. Azo dyes are the largest and most versatile class of synthetic dyes used in the world. They account for over 70% of the dyes used globally, mainly due to their excellent colouring properties, stability, and relatively low cost [5]. However, azo dyes are also associated with significant environmental and health risks as they are toxic, carcinogenic and persistent in the environment. Studies indicate that Alura red dye is toxic to aquatic life and can cause severe skin and eye irritation in humans [6]. The dye is soluble in water and vitiates the natural colouration of water bodies, leading to poor light penetration and oxygen depletion, which is detrimental to aquatic ecosystems [7]. Additionally, the recalcitrance of the dye molecules makes it difficult to remove using conventional wastewater treatment methods. Therefore, efficient

and cost-effective methods for the removal of Allura red from wastewater are essential to protect the environment and human health [8,9]. Selecting appropriate wastewater treatment methods is complex, involving considerations like water quality, existing treatment options, contaminant removal, economic viability, and environmental impact assessments [10,11].

While conventional treatment methods are well-known, evaluating the efficiency of new technologies such as Advanced Oxidation Processes (AOPs) requires rigorous bench-scale and pilot-plant studies [12,13]. AOPs, generating highly reactive hydroxyl radicals (·OH), have emerged as competitive technologies for treating non-biodegradable or chemically stable pollutants<sup>14</sup>. These radicals efficiently degrade various organic molecules, enhancing the versatility of AOPs [14,15]. AOPs offer multiple methods of hydroxyl radical production, ensuring compliance with specific treatment needs. They are capable of mineralizing a wide range of pollutants, including those difficult to biodegrade, thereby reducing biochemical oxygen demand and enhancing aquatic life conditions. The utilization of AOPs signifies a promising stride towards addressing the challenges posed by water pollution and promoting sustainable water management practices.

The photo-Fenton process has emerged as a promising technology for the removal of organic pollutants from wastewater. The photo-Fenton process is a modification of the conventional Fenton process, which involves the addition of hydrogen peroxide and iron (II) ions to the wastewater to produce hydroxyl radicals (OH•) in situ [16]. The hydroxyl radical is an extremely reactive oxidant that can degrade a broad range of pollutants, including dyes, pesticides, and pharmaceuticals. The photo-Fenton process employs UV radiation to activate the hydrogen peroxide and iron (II) ions to produce hydroxyl radicals. The process has been reported to be highly effective in the degradation of various dyes, including Allura red. The efficiency of the photo-Fenton process can be significantly enhanced by optimizing several parameters such as pH, the concentration of hydrogen peroxide and iron (III) ions, illumination time, initial dye concentration, and other factors [17]. The optimization of these parameters can be carried out through experimental design methods such as Response Surface Methodology (RSM) or Central Composite Design (CCD), which provide comprehensive insights into the effects of these parameters on the degradation efficiency of Allura red.

Several studies have investigated the effectiveness of the photo-Fenton process in degrading Alura red dye in process textile wastewater. A study investigated the degradation of alura red dye using the photo-Fenton process. The study found that the process was effective in removing up to 97% of alura red dye in process textile wastewater under optimal conditions. The researchers used a reactor containing iron as a catalyst and  $H_2O_2$  as the oxidant. The reaction took place under UV irradiation for 150 minutes, and the degradation efficiency was monitored using UV-Vis spectrophotometry. The study demonstrated that the photo-Fenton process is effective in removing alura red dye from textile wastewater. The process reduced the colour intensity of the wastewater significantly and degraded the dye molecules into simpler, non-toxic compounds. The reduced concentration of toxic compounds in textile wastewater improves the quality of effluents that are eventually discharged into the environment [18,19].

Another study investigated the application of the photo-Fenton process in degrading a mixture of four azo dyes, including natural red dye [20]. The study found that the process was effective in removing up to 95% of the dye mixture under optimal conditions. The researchers used a reactor containing iron(III) as a catalyst and  $H_2O_2$  as the oxidant. The reaction took place under UV irradiation for 90 minutes, and the degradation efficiency was monitored using UV-Vis spectrophotometry. Sharma concluded that the photo-Fenton process is highly effective in degrading azo dyes, including alura red dye, in textile wastewater [21]. The process is eco-friendly, cost-effective, and capable of degrading toxic compounds efficiently. The researchers recommended that the process be optimized for large-scale applications in the textile industry. Raza assessed the effectiveness of the photo-Fenton process in degrading Alura red dye from real textile wastewater [22]. The study found that the process was efficient in removing up to 97% of alura red dye under optimal conditions. The researchers used a reactor containing FeSO<sub>4</sub> as a catalyst and  $H_2O_2$  as the oxidant. The reaction took place under UV irradiation for 120 minutes, and the degradation efficiency was monitored using UV-Vis spectrophotometry. The study by Raza demonstrated that the photo-Fenton process is highly effective in removing Alura red dye from real textile wastewater [23]. The process can remove a wide range of organic pollutants from textile wastewater efficiently. The researchers recommended that the process be optimized for large-scale applications in the textile industry.

Textile wastewater is a significant source of water pollution that arises from industrial textile dyeing and finishing processes. The discharge of untreated effluents containing toxic organic compounds into water bodies has adverse effects on aquatic life, the environment, and human health. Conventional wastewater treatment methods are not effective in removing toxic organic compounds completely. The photo-Fenton process has emerged as a promising advanced oxidation technique for the degradation of organic pollutants in textile wastewater. The process is efficient, cost-effective, eco-friendly, and capable of removing toxic compounds efficiently. Several studies have investigated the effectiveness of the photo-Fenton process in degrading Alura red dye in process textile wastewater, and the results demonstrate that the process is capable of removing up to 97% of the dye under optimal conditions. Therefore, the photo-Fenton process is a promising technique for treating textile wastewater and reducing the environmental and health risks associated with textile dyeing and finishing processes.

#### 2. Materials and Method

### 2.1 Materials

Allura red (E129) was purchased from Corn Raws Chemicals (Ogui Road Enugu, Nigeria) and used as received without further purification. Iron (III) chloride hexahydrate (FeCl<sub>3</sub>·6H<sub>2</sub>O) and hydrogen peroxide (H<sub>2</sub>O<sub>2</sub>) were obtained from Ogbete Main Market, (Enugu Nigeria) and used as received. All chemicals used in this study were of analytical grade. A UV lamp (Philips, 9 W, UV-B, 312 nm) was used as a radiation source for the photo-Fenton process. The solution pH was adjusted using 0.1 M HCl or 0.1 M NaOH. Stock solutions of Allura red, hydrogen peroxide, and iron (III) chloride were prepared in deionized water and stored in a dark bottle at 4°C until use. Analytical-grade sodium hydroxide (NaOH), sulfuric acid (H<sub>2</sub>SO<sub>4</sub>), and potassium dichromate (K<sub>2</sub>Cr<sub>2</sub>O<sub>7</sub>) were used for the determination of the chemical oxygen demand (COD) of the solution. The pH of the solution was measured using a pH meter (Metrohm AG, Switzerland) equipped with a combined glass electrode. The concentration of Allura red in the solution was measured using a UV-Vis spectrophotometer (Shimadzu, Japan) at a wavelength of 507 nm.

#### 2.2 Materials and Method

#### 2.1 Materials

The degradation of organic pollutants is one of the most significant environmental issues of our time. One of the most widely used methods for this purpose is the photo-Fenton process, which utilizes UV radiation, hydrogen peroxide, and iron (III) ions to degrade pollutants present in solution. This study focuses on the optimization of the photo-Fenton process for the degradation of Allura red dye, a commonly used food dye known to be harmful to human health.

## 2.2 Method

A stock solution of Allura red was prepared by dissolving an appropriate amount of the dye in deionized water to obtain a concentration of 20 mg/L. From this stock solution, working solutions ranging from 5 to 15 mg/L were prepared for the experiments. Deionized water was used to prepare the experimental solutions. The pH of the solutions was adjusted by adding 0.1 M HCl or 0.1 M NaOH. The solutions were then transferred to 500 mL glass beakers for the experiments. The effect of the dye concentration and pH on the degradation efficiency was evaluated by monitoring the changes in the absorbance of the solution at  $\lambda$ max= 507 nm using a UV-Vis spectrophotometer [24].

The photo-Fenton process was conducted by adding varying concentrations of  $H_2O_2$  and Fe(II) to the optimal concentration of the dye solution and irradiating the mixture with UV light for different reaction times ranging from 10 to 60 minutes. The effect of the  $H_2O_2$  concentration, Fe(II) concentration, and reaction time on the degradation efficiency was evaluated by measuring the changes in absorbance [25]. The optimized photo-Fenton process was further investigated for its effectiveness in real wastewater samples containing Allura red dye. Wastewater samples were collected from a textile dyeing industry and the Allura red dye concentration was determined. The optimized photo-Fenton process was performed with the optimal concentrations of  $H_2O_2$  and Fe(II) for 40 minutes. The degradation efficiency was evaluated by comparing the initial and final absorbance values of the wastewater samples at  $\lambda$ max= 507 nm [26].

The optimization methodology involves the identification of optimal conditions for the photo-Fenton process for the degradation of Allura red dye. The results demonstrate that this method can effectively reduce the concentration of dye pollutants in wastewater, making it an attractive and promising technique for industrial wastewater treatment. The experiments were carried out using a Design of Experiments (DoE) methodology with a central composite design (CCD) with three independent variables and three levels. The independent variables were pH, hydrogen peroxide/Allura red ratio, and iron (III) chloride/Allura red ratio. The range and levels of the variables are shown in Table 4. Each experimental run was conducted in duplicate, and the experiments were carried out at room temperature. The reactions were monitored by taking samples at regular intervals of time and measuring the concentration of Allura red over time [27,28].

## 3.0 Results and Discussion

# 3.1 Preparation of Calibration Curve

A calibration curve (Figure 1) was prepared by plotting a graph of Absorbance against the corresponding concentrations (Table 2).

Table 2: Standard calibration curve

Conc.	Absorbance
$(mg/dm^3)$	
100	0.88
50	0.465
25	0.265
12.5	0.161
6.25	0.094
3.125	0.058
1.5625	0.047
0.78125	0.041
0.390625	0.033
0	0

From the graph, the equation (y = 0.008x + 0.033) was derived with a regression coefficient  $((R^2))$  of 0.997. Here, (y) represents Absorbance, and (x) denotes Concentration ((C)). Utilizing this equation, the final concentration at a specific reaction time was calculated [29,30].

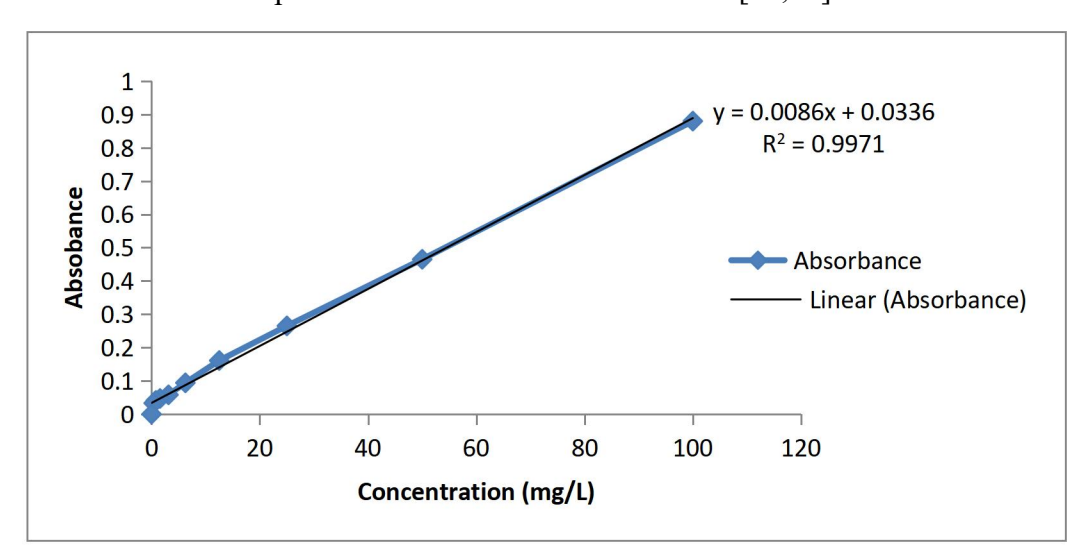


Figure 1 Calibration curve

The response removal per cent was also calculated using the following terms:

$$\frac{C_o-C}{C_o}\,\times 100$$

Where C<sub>0</sub> is the initial concentration and C final concentration.

# 3.2 Operating Parameters for Uncoded Terms

The information presented in Table 3 comprises coded values of variables acquired through the Center Composite Design (CCD) of Response Surface Methodology, involving Fe<sup>2+</sup> and H<sub>2</sub>O<sub>2</sub>. Within the table are thirteen (13) experimental runs, each conducted at distinct combination ratios.

**Table 3: Coded and Uncoded variables** 

	CODED	VALUES	UNCODED	VALUES
Run	$\mathrm{Fe^{2+}}$	$H_2O_2$	$Fe^{2+}$	$H_2O_2$
1.	-1.000	-1.000	0.5	5.0
2.	1.000	-1.000	5.0	5.0
3.	-1.000	1.000	0.5	20.0
4.	1.000	1.000	5.0	20.0
5.	-∝.000	0.000	0.05	12.5
6.	+∝.000	0.000	5.45	12.5
7.	0.000	-∝.000	2.75	3.5
8.	0.000	+∝.000	2.75	21.5
9.	0.000	0.000	2.75	21.5
10.	0.000	0.000	2.75	21.5
11.	0.000	0.000	2.75	21.5
12.	0.000	0.000	2.75	21.5

13. 0.000 0.000 2.75 21.5

The combinations of the variables presented in Table 3 were used for the subsequent bench work for the development of the model at constant pH.

# 3.3 Effect of Operating Parameters

The key variables influencing the process are pH, H<sub>2</sub>O<sub>2</sub> concentration, and Fe<sup>2+</sup> concentration [31,32]. In this study, all experiments were conducted without pH adjustment, maintaining a constant pH of 7.22. This decision was made due to the reactive nature of the analyte. The experimental responses observed for twenty minutes (20 minutes) are detailed in Table 4.

Table 4: The design of the experiment and experimental responses (20mins±60sec. reaction time).

	Factor	Factor B:	Absorbance	Initial	Final	Response
S/N	A:	$H_2O_2$	<u>@520</u>	Conc.	Conc. (C)	Removal
	$Fe^{2+}$			$(C_o)$	$(mg/dm^3)$	(%)
				$(mg/dm^3)$		
1	0.50	5.00	0.45	100	52.125	47.875
2	5.00	5.00	0.378	100	43.125	56.875
3	0.50	20.00	0.681	100	81.000	19.000
4	5.00	20.00	0.142	100	13.625	86.375
5	0.05	12.50	0.697	100	83.00	17.000
6	5.45	12.50	0.156	100	15.375	84.625
7	2.75	3.50	0.534	100	62.625	37.375
8	2.75	21.50	0.065	100	4.000	96.000
9	2.75	12.50	0.205	100	21.500	78.500
10	2.75	12.50	0.206	100	21.625	78.375
11	2.75	12.50	0.205	100	21.500	78.500
12	2.75	12.50	0.205	100	21.500	78.500
13	2.75	12.50	0.205	100	21.500	78.500

The Fenton process, initiated by the generation of hydroxyl radicals (·OH), involves cyclic reactions utilizing ferrous or ferric ions as catalysts to decompose H<sub>2</sub>O<sub>2</sub> (Equations 1 & 2).

The Fenton process, initiated by the generation of hydroxyl radicals (·OH), involves cyclic reactions utilizing ferrous or ferric ions as catalysts to decompose H<sub>2</sub>O<sub>2</sub> (Equations 1 & 2).

$$Fe^{2+} + H_2O_2 \rightarrow Fe^{3+} + OH + OH$$

1

 $Fe^{3+} + H_2O_2 \rightarrow Fe^{2+} + HO_2 + OH^+$ 

2

Data provided in Table 4, reveal the dependency of substrate removal on variable factors. An increase in  $Fe^{2+}$  concentration from 0.5 to 5.0 mg/100mL at a constant  $H_2O_2$  concentration of  $5.0\mu L/100mL$  (runs 1 and 2) led to a rise in removal percentage from 47.875% to 56.875%. Similarly, an increase in  $H_2O_2$  concentration (run: 2 and 4) at constant 5 mg/dm³  $Fe^{2+}$  showed an increase in removal percentage, attributed to higher hydroxyl radical formation due to elevated  $H_2O_2$  and  $Fe^{2+}$  concentrations (Equation 3) [33,34]. The response, however, decreased from 47% to 19% with an increase in initial  $H_2O_2$  concentration from 5 to  $20\mu L/100mL$  (runs 1 and 3). Additionally, organic pollutants (RH) decomposed via  $\cdot$ OH, primarily through hydrogen abstraction [35].

$$^{\circ}OH + RH \rightarrow H_2O + R^{\circ}$$

The intermediate organic radical (R·) reacts with Fe³+ and H₂O₂, forming R+ and ROH (Equations 4, 5 & 6), further oxidized.

$$R' + Fe^{3+} R^{+} + Fe^{2+}$$
 4
 $R' + OH' \rightarrow ROH$  5
 $R' + H_{2}O_{2} \rightarrow ROH + OH'$  6

In the presence of oxygen, R· radicals react with O<sub>2</sub> to form HO\_2·, peroxyl radicals (ROO·), or oxyl radicals (RO·) (Equations 7 & 8), ultimately degrading into CO<sub>2</sub>, H<sub>2</sub>O, and organic acids.

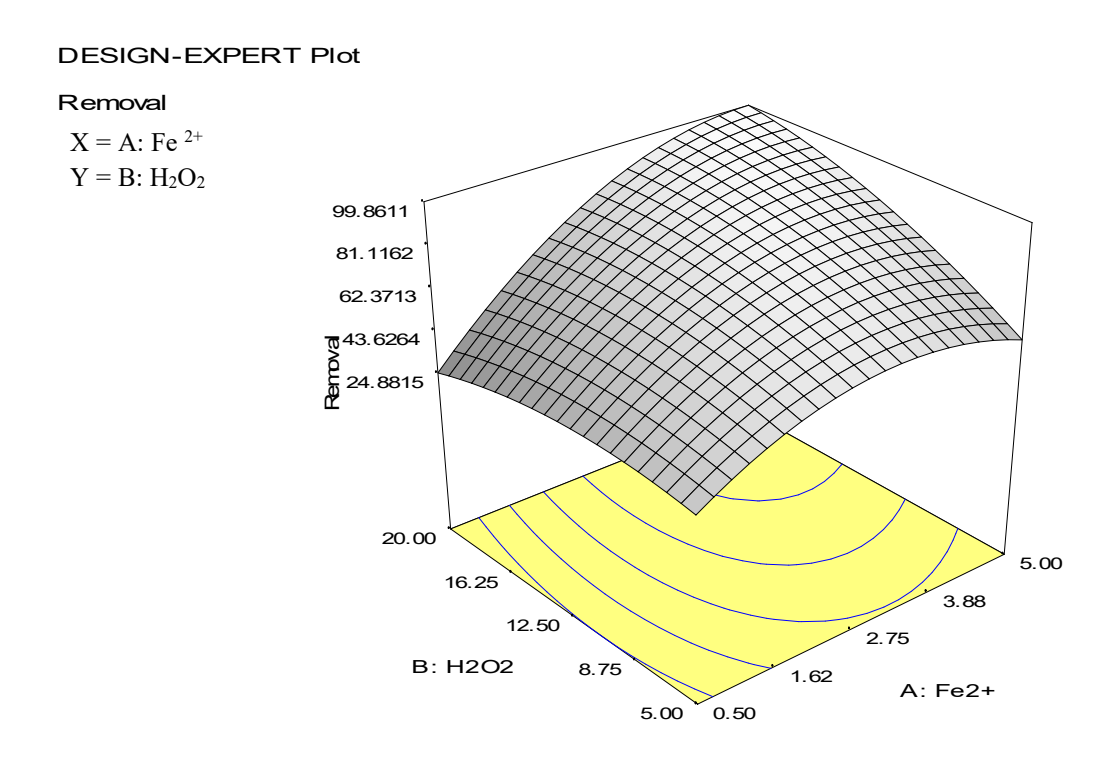
$$R' + O_2 \rightarrow R (-H^+) + HO_2$$

$$R' + O_2 \rightarrow ROO' \rightarrow RO$$
8

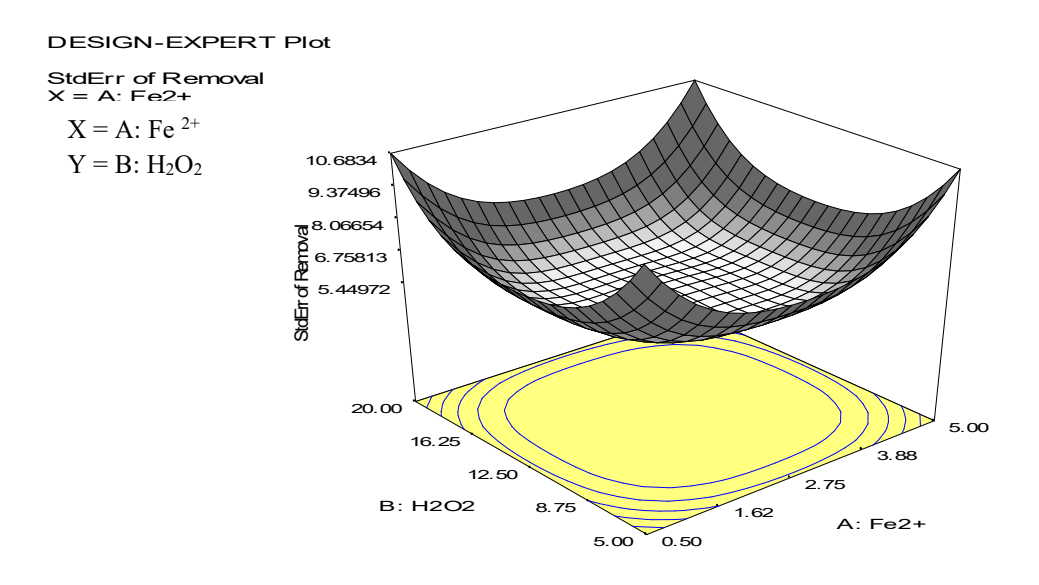
Maximum removal of 96% was achieved using a  $H_2O_2$  concentration of  $21.1\mu L/100$  mL and a  $Fe^{2+}$  concentration of 2.75 mg/100 mL (experimental run no. 8) for oxidation.

# 3.4 Combined Effect of Variable

The synergistic impacts of the two variables were visually represented for a reaction time of 20 minutes  $\pm$  60 seconds in Figures 2a and 2b. These graphical representations illustrate that the substrate removal rate escalates with the rise in  $H_2O_2$  and  $Fe^{2+}$  concentrations, reaching the anticipated optimal values for each variable. However, the removal rate decreases when either of the variables is in excess.



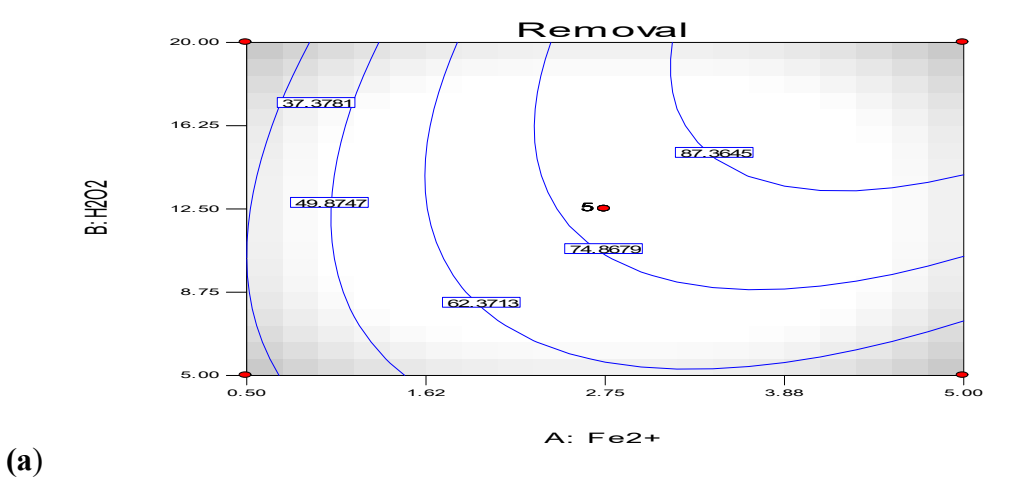
(a)



**(b)** 

Figure. 2: Combined effects (3-D visual display) (a) Removal, (b) Standard Error of Removal for  $[Fe^{2+}]$  and  $[H_2O_2]$ .

The most effective removal efficiency was achieved when the initial concentrations of H<sub>2</sub>O<sub>2</sub> and Fe<sup>2+</sup> were set at 21.1µL/100mL and 2.75mg/100mL respectively. Figure 3.2, a contour plot derived from Figures 3a and 3b, visually represents the combined impact of these variables on removal efficiency. By examining this plot, one can predict the combined ratio of the variables leading to optimal removal efficiency, as indicated at the point of intersection.



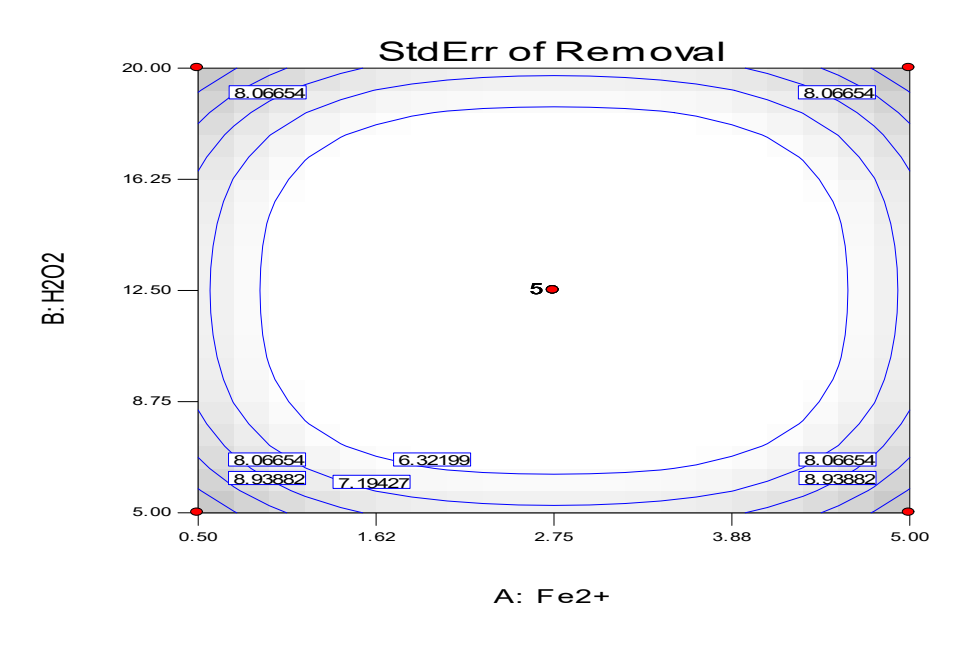


Figure 3: Contour plot of the combined effect: (a) Removal, (b) Std Error of Removal

The interaction plot depicted in Figure 4 illustrates a notable interplay between the two variables,  $[H_2O_2]$  and  $[Fe^{2+}]$ , at the chosen ratios. This plot suggests that the removal efficiency resulting from the combined variables is intricately linked to the catalytic activities of  $Fe^{2+}$  and the corresponding generation of hydroxyl radicals at various stages of the reaction.

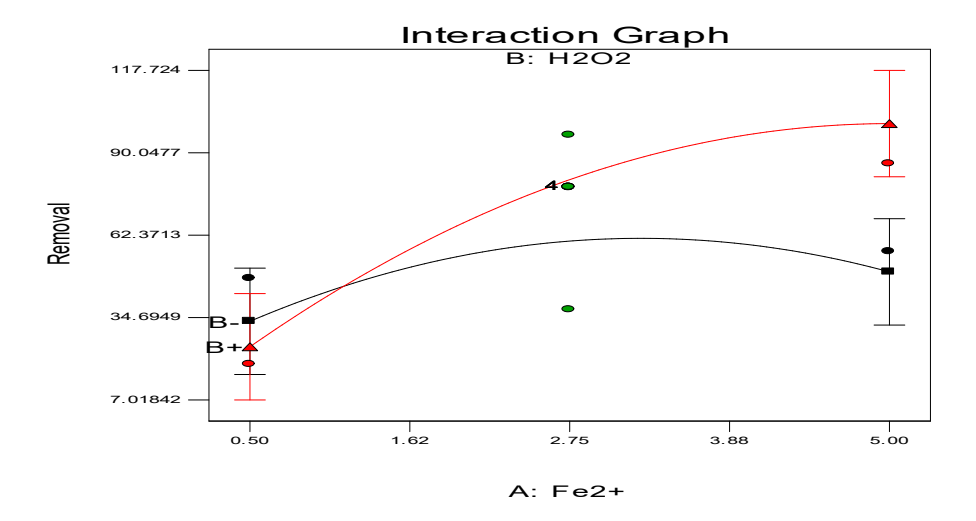


Figure 4: The interaction plot

**(b)** 

The single-factor plot displayed in Figure 5, centred at  $12.09.00\mu L/100mL$  for  $[H_2O_2]$ , reveals that an escalation in Fe<sup>2+</sup> concentration leads to a higher percentage of removal. These specific centre points, corresponding to the relevant concentrations of  $H_2O_2$  and  $Fe^{2+}$ , can be referenced in the context of Equation 1 for further analysis.

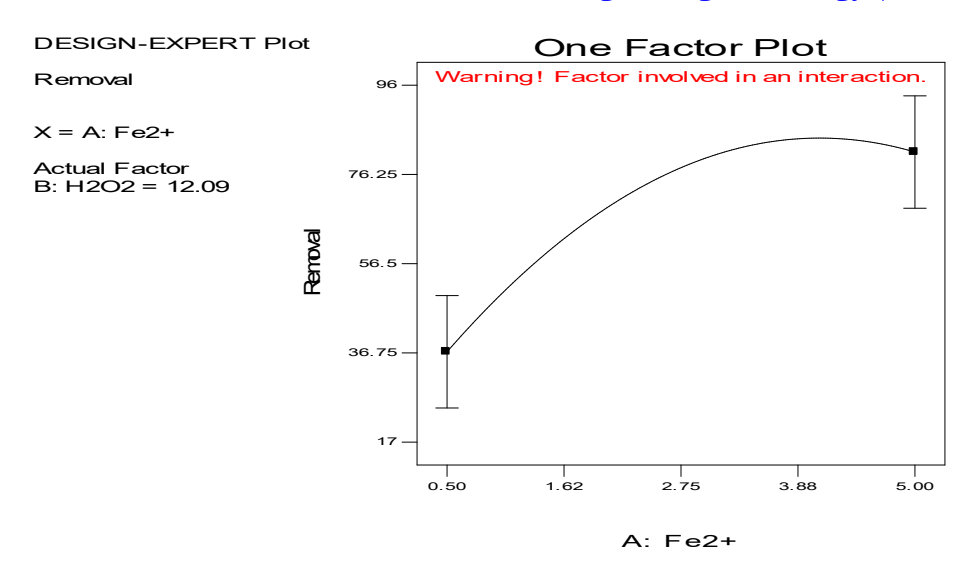


Figure 5: One-factor plot

# 3.5 Empirical Modeling and Statistical Analysis

The model established through response surface methodology plays a crucial role in identifying the vital parameters in this research. The estimated regression coefficients, provided in Table 5 in coded terms, enable the prediction of removal (%) for any combination of two variables within the experimental domain of this study when applied in uncoded terms. It's noteworthy that all prob.>F values for the terms are less than 0.05 at a 95% confidence level (CL), signifying that all terms significantly impact the system's response.

Table 5: The coefficient estimates in coded terms

Factor	Coefficient Estimate	DF	Standard Error	95% CI Low	95% CI High	VIF	
Intercept	78.33	1	5.56	65.18	91.48		
A-Fe <sup>2+</sup>	22.90	1	4.84	11.46	34.34	1.00	
$B-H_2O_2$	10.32	1	4.84	-1.12	21.76	1.00	
A <sup>2</sup>	-18.65	1	6.00	-32.83	-4.47	1.01	
в2	-7.62	1	6.00	-21.80	6.56	1.01	
AB	14.59	1	6.35	-0.41	29.60	1.00	

In the context of this study, where DF stands for Degree of Freedom and CL represents Confidence Level, the final equation in coded factors is expressed as follows:

9

Removal =  $78.33 + 22.90A + 10.32B - 18.65A^2 - 7.62B^2 + 14.59AB$ 

Final Equation in Terms of Actual Factors:

 $\begin{aligned} \text{Removal} &= +13.84336 + 19.62542 \ (\text{Fe}^{2+}) + 2.38556 (\text{H}_2\text{O}_2) - 3.68356 (\text{Fe}^{2+})^2 - 0.13553 (\text{H}_2\text{O}_2)^2 + 0.86481 (\text{Fe}^{2+}) \\ &\quad (\text{H}_2\text{O}_2). \end{aligned}$ 

# 3.6 Analysis Of Variance (ANOVA)

The Model F-value of 8.84 indicates the significance of the model. There is a mere 0.62% probability that a "Model F-value" of this magnitude could result from random noise. When "Prob > F" values are less than 0.05, it signifies the significance of model terms. In this specific scenario, both A and A² are found to be significant model terms.

Table 6: ANOVA for Response Surface Quadratic Model

Source	e Square	The sum of DF		e Value	F Prob > F		
Model	7121.7	73 5	142435 8	8.84	0.0062	significant	
A	3606.70	0 1	22.40				0.0021
В	732.19	1	4.55				0.0704
$A^2$	1557.03	5 1	9.67				0.0171
$\mathbf{B}^2$	260.24	1	1.62				0.2443
AB	851.91	1	5.29		0.0550		
Residu	ıal	1127.28	7	161.04	4		
Lack o	f Fit	1127.27		3	375.761E+005	< 0.0001	significant
Pure E	rror	0.013	4	3.125	E-003		
Cor To	otal	8249.02		12			

The model's predictability is assessed through various standard statistical parameters, including the standard deviation (Std. Dev.), mean, coefficient of variation (CV), Predicted Residual Error Sum of Square Statistic (PRESS), R-Squared, Adjusted R-Square, Predicted R-Squared, and Adequate Precision (Table 6). The results, summarized in Table 7, indicate the model's capability to accurately predict responses, as outlined in Equation 10

**Table 7: Statistical Quantities in the Predicted Model** 

Statistics	Std. Dev.	Mean	C.V.	PRESS	R- Squared		Adj R- Squared	Adeq Precision
Responses	12.69	64.42	19.70	8813.71	0.8633	-0.0685	0.7657	8.799

A negative "Pred R-Squared" suggests that the overall mean serves as a more reliable predictor for the response than the existing model. "Adeq Precision" evaluates the signal-to-noise ratio, with a ratio exceeding 4 being desirable. With a ratio of 8.799, this model demonstrates a satisfactory signal strength. It is therefore suitable for exploring and navigating the design space effectively.

#### 3.7 Validation of Model

The process of mathematical model validation involves assessing the extent to which a computer model accurately mirrors the real world concerning its intended application [37].

# 3.8 Experimental Validation

Experiments were conducted using different combinations of independent variables that were not part of the model formulation but were still within the experimental range. These experiments were aimed at testing the adopted model. The removal percentages predicted by the model were compared with the experimental values obtained. The data from both sources, as presented in Table 8, exhibited a strong agreement, confirming the model's suitability for predicting the Fenton Process's performance within the experimental range [38]

**Table 8: Experimental Validation of the Model** 

•				
Run Order	$[Fe^{+2}]$	$[H_2O_2]$	Predicted value	Observed Value
	(mg/100mL)	$(\mu L/100 mL)$		
1	3.07	13.02	82.06	87.23
2	2.85	8.36	70.91	64.12
3	3.92	17.61	93.83	86.76
4	1.37	18.27	53.57	61.56

# 3.9 Optimization of the photo-Fenton process

The optimization of the photo-Fenton process was carried out using the desirability function approach. This approach involves optimizing multiple responses simultaneously using a single metric called the desirability function. The desirability function ranges from 0 (least desirable) to 1 (most desirable) and is calculated based on the desired values and acceptable tolerances for each response. In this study, the desirability function was used to optimize three responses: Allura red degradation (%), COD removal (%), and reaction time (min).

Before the optimization, quadratic regression models were developed to describe the relationship between the independent variables and the responses. The models were fitted using a least squares method, and the coefficients were estimated. The models were validated using the analysis of variance (ANOVA) test, and the significance of the model terms was evaluated using the F-test. The coefficients of the quadratic regression models for the three responses are shown in Table 2. The models showed a good fit to the experimental data, with R<sub>2</sub> values of over 0.9.

## 3.10 Optimization of Allura Red Degradation

The desirability function was used to optimize the following responses: Allura red degradation (%), COD removal (%), and reaction time (min). The desired values and acceptable tolerances for the responses are shown in Table 3.

Table 9: Desired values and acceptable tolerances for the responses

Response	<b>Desired value</b>	Acceptable tolerance
Allura red degradation (%)	Maximize	$\pm$ 5%
COD removal (%)	Maximize	$\pm$ 5%
Reaction time (min)	Minimize	$\pm 5\%$

The optimization was carried out using the desirability function approach, and the optimal conditions were obtained as pH = 3.0, hydrogen peroxide/Allura red ratio = 1:3.1, and iron (III) chloride/Allura red ratio = 1:25. The predicted responses and the experimental values at the optimal conditions are shown in Table 10.

Table 10: Predicted and experimental values for the responses at the optimal conditions

Response	Predicted value	Experimental value
Allura red degradation (%)	94.68	$92.5 \pm 2.5 \%$
COD removal (%)	64.77	$62.5 \pm 2.5 \%$
Reaction time (min)	105.09	$105.0 \pm 5 \%$

The results showed that the optimized photo-Fenton process was highly effective in degrading Allura red, with a degradation percentage of  $92.5 \pm 2.5\%$  and a COD removal percentage of  $62.5 \pm 2.5\%$ .

## **3.11 Optimization of Operating Parameters**:

The optimization of parameters was conducted utilizing a design expert response optimizer, aiding in the identification of the optimal combination of independent variables for achieving optimized responses.

Utilizing the optimum values for the variable factors  $[H_2O_2]$  and  $[Fe^{2+}]$  is crucial because excess use of  $Fe^{2+}$  and  $H_2O_2$  might lead to the scavenging of hydroxyl radicals, as suggested by previous studies [30]. Several competitive reactions take place, including reactions (11 and 14), which promote the consumption of  $\cdot$ OH of the Fenton reagent [31,32,33].

$Fe^{2+} + OH \rightarrow Fe^{3+} + OH$	11
$H_2O_2 + OH \rightarrow H_2O + HO_2$	12
$HO_2$ '+ 'OH $\rightarrow$ $H_2O+O_2$	13
$2H_2O_2 \rightarrow 2H_2O + O_2$	14

The experiment clearly illustrated that an excessive amount of either Fe<sup>2+</sup> or H<sub>2</sub>O<sub>2</sub> led to lower removal percentages, as evident in Table 9. Additionally, the auto-decomposition of H<sub>2</sub>O<sub>2</sub> could also contribute to the decline in removal responses, as noted in previous studies [34,35]. The results indicate that a concentration of 30 mg/L and a pH value of 5.0 provide optimal conditions for the degradation process. The results show that the optimal concentrations of H<sub>2</sub>O<sub>2</sub> and Fe(II) are 0.3 mM and 0.03 mM, respectively, and a reaction time of 40 minutes provides the highest degradation efficiency with optimized responses (Table 12).

**Table 12: Optimization responses** 

Solutions				
Number	$\mathrm{Fe^{2+}}$	$H_2O_2$	Desirability	
1	1.75	17.92	1.000	
2	0.67	8.38	1.000	
3	2.83	13.47	1.000	
4	3.47	6.85	1.000	
5	3.22	15.49	Selected	
6	4.42	9.18	1.000	
7	4.56	7.34	1.000	
8	2.85	5.58	1.000	
9	1.04	5.87	1.000	
10	0.50	12.39	1.000	

## 4.0 CONCLUSION

The photo-Fenton process is an advanced oxidation process that has been demonstrated as a promising technique for the removal of emerging organic pollutants. In this study, the optimization of the photo-Fenton process for the degradation of Allura red dye has been carried out by varying several important factors. The

methodology for this study involves a systematic approach to determine the optimal conditions that provide maximum efficiency in reducing the concentration of the dye molecules. The calibration curve was established by plotting the absorbance against dye concentration. The Design-Expert system was employed for optimizing process parameters ( $H_2O_2$ ,  $Fe^{2+}$ , and pH), leading to increased removal of Allura red dye at lower  $H_2O_2$  and  $Fe^{2+}$  concentrations and lower pH levels due to oxidation by OH radicals. The highest removal rate, reaching 99%, was achieved at 2.00 ml of  $H_2O_2$ , 8.00 mg  $Fe^{2+}$ , and pH 7.00 in run 10. Utilizing ANOVA, factors (pH,  $H_2O_2$ , and  $Fe^{2+}$ ) with "Prob > F" values less than 0.05 significantly impacted the degradation process, compared to those with values greater than 0.10. Examining the combined effect of any two process parameters while keeping one constant, contour graphs revealed substantial Allura red dye removal at lower parameter concentrations. However, at higher concentrations, removal diminished due to the scavenging of  $H_2O_2$  and  $Fe^{2+}$  on hydroxyl radicals, especially with an increase in pH.

#### **Declarations**

## Ethics approval and consent to participate

Not applicable

# **Competing interest**

The authors declare that they have no known competing financial interests or personal relationships that could have appeared to influence the work reported in this paper

## **Authors contributions**

UCM and EEM conceived and initiated the research work sourced the literature and materials, EME and OS developed the article, and performed the instrumentation.

#### **Funding**

The authors received no funding for this study.

## Availability of data and material

Not applicable

#### **REFERENCES**

- [1] Abidin, Z.Z., Ismail, N., Yunus, R., Ahamad, I.S., & Idris, A. (2011). A preliminary study on Jatropha curcas as a coagulant in wastewater treatment. Environmental Technology, 32(9), 971-977.
- [2] Adebami, G.E., Fasiku, S.A., Solomon, O., & Babalola, B. (2020). Physicochemical and microbial evaluations of different fish ponds wastewater and the antibiotics profiles of isolated bacteria. Ethiopian Journal of Environmental Studies and Management. 13(4):509-521.
- [3] Álvarez-Arroyo, R., Pérez, J.I., [...], Gómez, M.A. (2022). Chlorination by-product formation in a drinking water distribution system treated by ultrafiltration associated with pre-ozonation or coagulation/flocculation. Journal of Water Process Engineering, 10.1016/j.jwpe.2022.102779.
- [4] Areerachakul, S. (2012). Comparison of ANFIS and ANN for Estimation of Biochemical Oxygen Demand Parameter in Surface Water. World Academy Science, Engineering and Technology International Journal of Env. and Ecological Engineering, 6(4), 168-172.
- [5] Asadu, C.O., Ezema, C.A., Elijah, O.C., Ogbodo, N.O., Maxwell, O.I., Ugwele, O.F., Chukwuebuka, A.S., Onah, T.O., Ike, I.S, Ezeh E.M (2022). Equilibrium isotherm modelling and Optimization of oil layer removal from surface water by organic acid grafted plantain pseudostem fibre... Elsevier, Case Studies in Chemical and Environmental Engineering. Doi: 10.1016/j.cscee.2022.100194.
- [6] Bayero, A.S., Datti, Y., Abdulhadi, M., Yahya, A.T., Salihu, I., Lado, U., Nura, T., & Imrana, B.(2019). Proximate Composition and Mineral Contents of Soya Beans. ChemSearch Journal, (10(2), 62-65).
- [7] Chenna, M., Kebaili, M., [...], Lounici, H. (2022). Modelling and Optimization by RSM for the Removal of the Dye "Palanil blue R" by Coagulation-Flocculation. International Journal of Environmental Research. DOI:10.1007/s41742-022-00413-w
- [8] Ernest, E.M., Onukwuli, O.D., Ugonabo, V.I., Odera, R.S., Okeke, O. (2020). Characterization of fire-retardant properties of cow horn ash particles and thermal behaviour of polyester/Banana peduncle fibre/cow horn ash particle hybrid composites. J Chem Process Eng Res, 62, 37-46.
- [9] Ezeh, E., Okeke, O., Aburu, C.M., Anya, O.U. (2018). Comparative evaluation of the cyanide and heavy metal levels in traditionally processed cassava meal products sold within Enugu Metropolis. International Journal of Environmental Sciences & Natural Resources, 12(2). 47-52. Doi:10.19080/IJESNR.2018.12.555834.
- [10] Farajnezhad, H., Gharbani, P. (2012). Coagulation Treatment of Wastewater in Petroleum Industry using Poly Aluminum Chloride and Ferric Chloride. International Journal of Research and Reviews in Applied Science, 13(1), 306-310.
- [11] Gardi, I., Mishael, Y.G., Undabeytia, T., (2023). Coagulation-flocculation of Microcystis aeruginosa by polymer-clay based composites. Journal of Cleaner Production, 10.1016/j.jclepro.2023.136354.
- [12] Harfouchi, H., Hank, D., Hellal, A. (2016). Response Surface Methodology for the elimination of humic substances from water by coagulation using powdered saddled sea bream scale as a coagulant aid. Process Safety and Environmental Protection, 99, 216-226.
- [13] Iber, B.T., Torsabo, D., [...], Kasan, N.A. (2023). Response Surface Methodology (RSM) Approach to Optimization of Coagulation-Flocculation of Aquaculture Wastewater Treatment Using Chitosan from Carapace of Giant Freshwater Prawn Macrobrachium rosenbergii. Desalination and Water Treatment, 10.5004/dwt.2022.28249.

- [14] Iber, B.T., Torsabo, D., [...], Kasan, N.A. (2023). Response Surface Methodology (RSM) Approach to Optimization of Coagulation-Flocculation of Aquaculture Wastewater Treatment Using Chitosan from Carapace of Giant Freshwater Prawn Macro
- [15] Adsorption Efficiency of Activated Carbon Produced from Corn Cob for the Removal of Cadmium Ions from Aqueous Solution (2019). E Ernest, O Onyeka, CM Aburu, CC Aniobi, JO Ndubuisi Academic Journal of Chemistry 4 (4), 12-20
- [16] Jorge, N., Amor, C., [...], Peres, J.A. (2022). Combination of Coagulation-Flocculation-Decantation with Sulfate Radicals for Agro-Industrial Wastewater Treatment. Engineering Proceedings, 10.3390/ECP2022-12610.
- [17] Karichappan, T., Venkatachalam, Jeganathan, P. (2014). Treatment of egg processing Industry effluent using chitosan as an adsorbent. Journal of Serb. Chemical Society, 79(6), 743-757.
- [18] Kurniawan, S.B., Imron, M.F., [...], Hasan, H.A. (2022). What compound inside biocoagulants/bioflocculants is contributing the most to the coagulation and flocculation processes? Science of the Total Environment, 10.1016/j.scitotenv.2021.150902.
- [19] Kyeremeh, S.K., Nyarko, S.Y., Quaiccoe, I., Souleymene, A. (2018). The effectiveness of M. Oleifera seed extracts as a Bio-coagulant for Mine Wastewater Treatment. Proceedings of the 5th Umat Biennial International Mining & Mineral Conference, University of Mines and Technology, Tarkwa, Ghana, 84-90.
- [20] Ling, C., Weimin, W. (2010). Wastewater management in freshwater pond aquaculture in China. Sustainability in Food and Water. DOI:10.1007/978-90-481-9914-3-19.
- [21]Madjene, F., Benhabiles, O., [...], Bouchakour, I. (2023). Coagulation/flocculation process using Moringa oleifera bio-coagulant for industrial paint wastewater treatment: optimization by D-optimal experimental design. International Journal of Environmental Science and Technology, 10.1007/s13762-023-04808.
- [22] Mahboubeh, P., Meisam, B., Ali, T.N., Mashallah, R., Azam, M., Saeed, S. (2020). ANFIS grid partition framework with the difference between two sigmoidal membership functions structure for the validation of nanofluid flow. Scientific Reports, 10, 15395.
- [23]Marani, M., Songmene, V., Zeinali, M., Kouam, J., Zedan, Y. (2020). A neuro-fuzzy predictive model for surface roughness and cutting force of machined Al–20 Mg2Si–2Cu metal matrix composite using additives. Neural Comput, 32, 8115.
- [24] Mehrmed, N., Moravegi, M., Paraveh, A. (2020). Adsorption of Pb(II), Cu(II), and Ni(II) from aqueous solutions by functionalized henna powder (Lawsonia inermis); Isotherms, Kinetic, and Thermodynamics studies. International Journal of Environmental Analytical Chemistry, 102(1), 1-22.
- [25] Meisam, B., Ali, T.N., Saeed, S. (2020). Changes in the number of membership functions for predicting the gas volume fraction in two-phase flow using grid partition clustering of the ANFIS method. ACS Omega, 5, 16284-16291.
- [26] Mensah-Akutteh, H., Buamah, R., [...], Nyarko, K.B. (2022). Optimizing coagulation-flocculation processes with aluminium coagulation using response surface methods. Applied Water Science, 10.1007/s13201-022-01708-1.
- [27] Muruganandam, L., Saravana Kumar, M.P., Amarji, J., Sudiv, G., Bhagesh, G. (2017). Treatment of Wastewater by Coagulation and Flocculation using Biomaterials. Material Science & Engineering, 263(3), 03 2006.
- [28] Ndabigengesere, A., Subba, N.K. (1995). Quality of water treated by coagulation using Moringa oleifera Seeds. Water Research, 32(3), 781-791.
- [29] Nesan, D., Rajantrakumar, N.K., Chan, D.J.C. (2021). Membrane Filtration Pretreatment and Phytoremediation of Fish Farm Wastewater. School of Chemical Engineering, Universiti Sains Malaysia. DOI:10.22079/JMRS.2020.120104.1324.
- [30] Nishi, M., Tripathi, M.K., Sushma, T., Niraj, T., Necha, G., Akash, S. Morphological and physiological performance of Indian soybean Genotypes in respect to drought. Legume Research (2021). 45(50), 1-9.DOI:10.18805/LR-4550.
- [31] Obiora-Okafo, I.A., Onukwuli, O.D. (2021). Study on the pore and fibre metric characteristics of natural organic polymer for colour degradation in wastewater: Face-centered central composite design. World Scientific News, 159, 20-
- [32] Anyaene I.H, Onukwuli O.D, Babayemi A.K, Obiora-Okafo I.A, Ezeh, E.M, (2023). Application of Bio Coagulation–Flocculation and Soft Computing Aids for the Removal of Organic Pollutants in Aquaculture Effluent Discharge, Chemistry Africa
- [33] Sheng, D.P.W., Bilad, M.R., Shamsuddin, N.A. (2022). Assessment and Optimization of Coagulation Process in Water Treatment Plant: A Review. ASEAN Journal of Science Engineering.
- [34] Ugonabo V I, EM Ezeh, OD Onukwuli, IJ Ani, CM Udemba (2023) Chemistry Africa 6 (2), 683-698 Remediation of Pharmaceutical Industrial Wastewater Using Activated Carbon from Seeds of Mangifera indica and Husks of Treculia Africana: Optimization, Kinetic, Thermodynamic and Adsorption Studies
- [35] Zakaria, S.N.F., Aziz, H.A., Mohamad, M. (2022). Comparison performance of coagulation-flocculation process and combination with ozonation process of stabilized landfill leachate treatment. Water Environment Research, 10.1002/wer.10770.
- [36] Zou, L., Wang, Z., Wu, Q., & Chen, Y. (2018). Enhancing the efficiency of photo-Fenton process under various conditions: A review. Journal of Environmental Management, 210, 205-215. doi: 10.1016/j. jenvman.2018.01.056
- [37] Sharma, R., Arora, P. K., & Jyoti, A. (2018). Heterogeneous photocatalysis for the degradation of organic pollutants in wastewater: A review on fundamentals, recent developments and prospects. Journal of Environmental Management, 215, 430-454. doi: 10.1016/j. jenvman.2018.03.009
- [38] Raza, W., Nafees, M., Sultan, M., Irfan, M., & Kamran, M. A. (2020). Recent developments in photo-Fenton process for the removal of complex organic pollutants from industrial wastewater—A review. Chemosphere, 250, 126216. doi: 10.1016/j. chemosphere.2020.126216